Research Article

Xuya Fu[#], Tao Zhang*[#], Wenshuo Zhang, Yuye Zhong, Shuliang Fang, Guannan Wang, Ying Li, Yajun Deng, Xinghai Liu, and Houbin Li*

Melt-blended PLA/curcumin-cross-linked polyurethane film for enhanced UV-shielding ability

https://doi.org/10.1515/epoly-2023-0009
received February 01, 2023; accepted March 26, 2023

Abstract: Biomass films with ultraviolet (UV)-shielding ability have attracted considerable attention. Curcumin was introduced into castor oil-based polyurethane (CCPU) as a chain extender, which was melt with polylactic acid (PLA) as a reinforcement to obtain biomass UV-shielding film. The excellent UV absorption and antioxidant qualities of curcumin contributed to the impressive UV-shielding capacity (97.6% UV radiation absorption) and antioxidant (51% free radical scavenging) of PLA/CCPU-20 film. In the scanning electron microscopic images of film fracture, the mixing of CCPU elastomer into the PLA matrix caused the blend films to exhibit significant toughening fracture characteristics compared to the pure PLA film. The excellent thermal stability, low water swelling degree, and low water solubility of PLA/CCPU blend films were maintained after CCPU was added to the PLA matrix. Therefore, the PLA/CCPU blend films can be considered as a potential packaging material because of its favorable UV-shielding properties and film stability.

Keywords: polylactic acid, polyurethane, curcumin, UV-shielding, melt mixing

1 Introduction

Food and organic industrial products may deteriorate or age if directly exposed to ultraviolet (UV) light (1–5). Traditional packaging and coating materials such as rubber, plexiglas, paints, dyes, and paper often focus only on mechanical properties and overlook the damage of UV rays (6), which will greatly affect the beauty and safety of the product. Research into packaging materials with UV-shielding capabilities is urgently needed. On the other hand, functional biomass materials are constantly being proposed and improved in the hope of replacing traditional plastics (7,8). The large volume of plastic products used in the packaging industry per year has accelerated the depletion of fossil resources and caused uncontrollable environmental pollution problems (9,10). Therefore, it is particularly important to more actively use biomass materials as substrates to prepare UV-shielding blend (composite) films that can absorb UV radiation.

In recent years, functional biomass fillers with UV-shielding properties have been intensively researched (11). It was found that the main components of some renewable natural resources, such as phenols and ketones (12), can effectively block UV radiation. Common biomass materials with UV absorption capacity include lignin (13–15), amaranth (16), curcumin (17), and grape seed (18). In particular, curcumin is an easily available hydroxyl-terminated natural compound that can be isolated from the plant *Curcuma longa* and used as a phyto-polyphenol pigment, which is safe and nontoxic and has excellent antioxidant and antibacterial properties (19–21). Curcumin is a diketone natural pigment with both benzene ring and

# These authors contributed equally to this work.

*** Corresponding author: Tao Zhang,** Research Center of Graphic Communication, Printing and Packaging, Wuhan University, Wuhan, 430079, China, e-mail: zt2022dyj@whu.edu.cn
*** Corresponding author: Houbin Li,** Research Center of Graphic Communication, Printing and Packaging, Wuhan University, Wuhan, 430079, China, e-mail: lhb@whu.edu.cn
Xuya Fu, Wenshuo Zhang, Yuye Zhong, Ying Li, Xinghai Liu: Research Center of Graphic Communication, Printing and Packaging, Wuhan University, Wuhan, 430079, China
Shuliang Fang: China Helicopter Research and Development Institute, Jingdezhen, 333001, China
Guannan Wang: Food Science Institute, Zhejiang Academy of Agricultural Sciences, Hangzhou, 310021, China
Yajun Deng: Jimei University, Xiamen Key Laboratory of Marine Corrosion and Intelligent Protection Materials, Xiamen, Fujian 361021, China

ketone carbonyl structures in its molecular structure, and benefiting from the combined action of adjacent carbon–-carbon double bonds and carbonyl groups, curcumin can effectively absorb a wide range of UV rays (22,23). However, the absorption of UV radiation by curcumin also imposes limitations on its bioavailability, and curcumin is extremely unstable under sunlight when used alone (24,25). Surprisingly, the preparation and application of curcumin-based biomass materials may be a way to alleviate this limitation. Several studies (26,27) have shown that grafting small molecules onto the backbone or side chains of polymers is an innovative strategy to obtain the functional polymers. Curcumin can be introduced into polyurethane (PU) molecules as a chain extender through the reaction of the terminal hydroxyl group with the isocyanate group (–NCO) without destroying the benzene ring and ketone carbonyl structure of curcumin itself (28), which means that the UV-shielding ability of curcumin can be retained after the chemical crosslinking (29,30). Curcumin-based PU is an environment-friendly material that can be greatly used as a blend component to toughen and modify conventional polymers (31–33). Furthermore, it has been documented that curcumin can be ideally dispersed during the preparation of curcumin-based PUs, thus avoiding the problem of poor utilization of curcumin due to potential agglomeration (34) and ensuring that curcumin can be firmly linked to the PU backbone, which in turn prevent a significant migration of curcumin (35–37). Therefore, it can be inferred that the stability of curcumin in curcumin-based PUs is also applicable to other blend systems in which polymers are mixed with curcumin-based PUs.

In the packaging, polylactic acid (PLA)-based materials with UV-shielding capabilities are also highly anticipated (38). PLA is derived from renewable resources (e.g., corn), and it is an easily accessible biomass material that is environment-friendly (39,40). In recent years, PLA has attracted a lot of attention from researchers because of its advantages such as excellent transparency, thermoplastics, and nontoxicity (41,42). However, the disadvantages of pure PLA, such as brittleness, limited ductility, and photodegradation of the pure PLA film under UV light, have restricted the promotion of PLA materials in packaging (43). Therefore, it is necessary to obtain PLA-based packaging, such as functional blend films, to handle the specific protection needs of different products (44–46). Blending pure PLA with functional fillers is one of the promising and effective methods to prepare the PLA-based blend films with UV-shielding capability (47–49).

Generally, the processing methods of PLA can be divided into two categories: dry processing and wet processing (50). In addition, the solution-casting method and melt co-mingling molding process are two more mature technological methods. Considering the disadvantages of the solution-casting method for the film production (51,52), such as long processing time, difficulty in controlling the volatilization of harmful solvent, and unsuitability for the large-scale industrial production, it may be more reasonable to use a more industrialized method for the film production. In some studies, melt mixing and compression molding have been indicated to have the potential to efficiently produce the PLA/PU uniform blends without excessive dependence on solvents (53,54). Therefore, preparing a curcumin-based PU and then compounding it with pure PLA by the melt co-mingling molding process (melt mixing and compression molding) is a worthwhile attempt to process UV-shielding films.

In summary, in this article, the PLA-based blend films containing 5, 15, and 20 wt% castor oil-based polyurethane (CCPU) were built by melt mixing and compression molding to block UV radiation. Furthermore, besides the desire to obtain better UV-shielding films compared to the pure PLA film, we also reported in detail the chemical properties, optical properties, mechanical properties, thermal stability, antioxidant activity, and water contact properties of the PLA/CCPU blend films which we wish to prepare to evaluate their potential usefulness.

2 Experimental section

2.1 Materials

PLA (Ingeo 4032D, M_n = 25,000 g·mol^{-1}) pellets were obtained from NatureWorks LLC (Minnesota, USA). Prior to melt compounding, PLA pellets were oven-dried at 80°C for 24 h. Castor oil (M_w = 933.44 g·mol^{-1}, USP), isophorone diisocyanate (IPDI, M_w = 222.28 g·mol^{-1}, ≥99%), and 2,2-diphenyl-1-picrylhydrazyl (DPPH, ≥97%, HPLC) were purchased from Aladdin (Shanghai, China) Co., Ltd. Curcumin ($C_{21}H_{20}O_6$, M_w = 368.38 g·mol^{-1}, ≥98%) and 1,4-butanediol (BDO, M_w = 90.12 g·mol^{-1}, ≥99%) were obtained from Adamas-beta. Acetone (≥99.5%, AR) and methanol (≥99.5%, AR) were available from Sinopharm Chemical Reagent Co., Ltd. Acetone was stored in a 4 Å molecular sieve for further use. All chemicals were used without additional purification.

2.2 Preparation of CCPU

The preparation methods of thermoplastic polyurethane (TPU) have been reported in several studies (55). In this article, it was first necessary to obtain CCPU that cross-

linked curcumin and to retain an excess of –NCO in the fabricated samples. Typically, IPDI (27 mmol, 6 g) and castor oil (10.7 mmol, 10 g) were added into a three-necked round-bottomed flask, stirred, and heated at a temperature of 80°C under nitrogen atmosphere for 2 h. Next, curcumin (0.8 mmol, 0.3 g) was added into the reaction for 1 h to help TPU exhibit a great UV-shielding ability. At this point, the addition of 5–10 mL acetone can help curcumin react more completely. Finally, the reaction was continued for 1 h using BDO (5.5 mmol, 0.5 g) as a chain extender for PU. The resulting viscous fluid was the CCPU. The nonreactive –NCO in the CCPU was retained with 9.3 mmol. The CCPU was cooled to room temperature under vacuum conditions, bottled and sealed, and stored in 4 Å molecular sieve for additional use.

2.3 Fabrication of PLA/CCPU blend films

The pure PLA melt and PLA/CCPU blends containing 5, 15, and 20 wt% CCPU were obtained by melt mixing in an internal mixer (SU-70; Suyan Science & Technology Co., Ltd, Changzhou, China). The rotation speed of the internal mixer was set at 30 rpm, and PLA was mixed with CCPU at 180°C for 15 min. Subsequently, the PLA/CCPU blends were pressed by a hot presser (R-3212; Wuhan Qien Science & Technology Development Co., Ltd, Wuhan, China) at 180°C and 10 MPa for 5 min, and the blend films were obtained from a mold (100 mm × 10 mm × 0.15 ± 0.05 mm) for characterization. The nomenclature of the PLA/CCPU blend films was abbreviated as PLA/CCPU-X, where X indicates the weight percentage of CCPU in the blend films (X includes 0, 5, 15, and 20).

3 Film testing and performance characterization

3.1 Fourier transform infrared (FT-IR)

The chemical analysis of the PLA/CCPU blend films was performed in the 4,000–300 cm^{-1} range using a spectrometer (Nicolet iS50, Thermo Scientific, Britain) in attenuated total reflection (ATR) infrared mode.

3.2 Scanning electron microscopy (SEM)

The cross-sectional morphology of the PLA/CCPU blend films was measured on an SEM (FEI Quanta 200, Netherlands). PLA/CCPU blend films that were treated with two different methods (cryo-fractured and tensile fracture) and sprayed with gold for 90 s were characterized at 5 kV under a high-vacuum mode. Images were captured at 1,000× magnification using SEM.

3.3 Ultraviolet-visible spectroscopy (UV-Vis)

The UV-shielding ability of the blend films was determined using an UV-Vis spectrometer (Ultrospec 2000; Scinteck, UK) in the wavelength range of 200–800 nm. The size of the film samples for testing was selected as 60 mm × 50 mm × 0.15 ± 0.05 mm.

3.4 Transmittance (*T*) and haze (*H*)

The *T* and *H* of the blend films were estimated using an optical tester (TH-09; Hangzhou Color Spectrum Technology Co., LTD, Hangzhou, China), according to ASTM D1003-00 (2000).

3.5 Thermogravimetry analysis (TGA)

The TGA of the blend films (10 mg) was performed in the range of 25–600°C on a TGA device (STA7300; Hitachi Limited, Japan), under N_2 atmosphere, whose flow rate was set as 20 $mL{\cdot}min^{-1}$ with a heating rate of 10°C·min^{-1}.

3.6 Mechanical properties

The tensile properties of the PLA/CCPU blend films were measured on a universal tensile tester (Instron 3343, USA), equipped with a 5 KN load cell and with a cross-head speed set as 1 $mm{\cdot}min^{-1}$. A suitable film size (55 mm × 5 mm × 0.15 ± 0.05 mm) was cut, and the distance between grips was set as 5 mm to test the tensile properties, according to ASTM D882-12.

3.7 Water contact angle (WCA)

The WCA of the blend films was recorded on an optical, high-speed, contact angle-measuring system (CAST3,

KINO, USA), and the images were acquired and evaluated by built-in software of the machine to estimate the surface wettability of films.

3.8 Swelling degree (SD) and solubility (*S*)

The SD and *S* of the blend films were estimated through Eqs. 1 and 2 (56). In the test, the film samples were first cut into pieces of a suitable size (1.5 cm × 1.5 cm) and dried at 105°C for 24 h (record the weight of the pieces as W_i). Then, the dry pieces were immersed in 40 mL of distilled water for 24 h, and the filter paper was used to discard the excess of liquid water before each weight (record the weight of the pieces as $W_{swollen}$). Finally, the pieces were dried again at 105°C for 24 h (record the weight of the pieces as W_s).

$$SD(\%) = \left(\frac{W_{swollen} - W_i}{W_i}\right) \times 100\% \quad (1)$$

$$S(\%) = \left(\frac{W_i - W_s}{W_i}\right) \times 100\% \quad (2)$$

3.9 Antioxidant activity of the films

The antioxidant activity of the blend films was measured by the DPPH free radical scavenging method (57). First, DPPH solution was prepared by dissolving 0.004% DPPH in methanol. Second, 50 mg of samples from each of the four films (PLA, PLA/CCPU-5, -15, and -20) was taken in four brown bottles containing 10 mL of DPPH solution and was incubated in the dark for 30 min, and then, the UV-vis absorbance of the four incubated solutions at 517 nm was measured using a UV-vis spectrophotometer (Ultrospec 2000; Scinteck, UK), and the data were recorded as A_1. The DPPH solution without the addition of sample was used as a control, and it was also tested at the UV-vis absorbance at 517 nm, and the data were recorded as A_0. Finally, the free radical scavenging rate was calculated using Eq. 3 to estimate the antioxidant activity of PLA/CCPU blend films:

$$\text{Free radical scavenging activity (\%)} = \frac{A_0 - A_1}{A_0} \times 100\% \quad (3)$$

where A_0 and A_1 represent the absorbance of the control group and the experimental group, respectively. Ideally, the test samples should be tested in triplicate.

4 Results and discussion

4.1 Chemical analysis

The chemical changes in the PLA/CCPU blend films were investigated by FT-IR-ATR. Spectra for the pure PLA film and PLA/CCPU blend films were collected as references to identify any differences. FT-IR spectra (Figure 1a) indicate that the N–H stretching vibration of CCPU, centered at around 3,421 cm^{-1}, exhibited a significant blue shift from 3,421 to 3,483 cm^{-1}. This is due to the interaction with the stretching vibration of the PLA ester O–H group and the CCPU ester N–H group (58). The stretching vibration of the PLA ester C═O groups at 1,758 cm^{-1} can be clearly identified from these PLA/CCPU blend films. Additionally, the amide bands (i.e., C═O stretching) at 1,636 cm^{-1} are also clearly visible in all of the PLA/CCPU blend films. The presence of these characteristic bands associated with amide groups confirms the existence of CCPU in the PLA/CCPU blend films (59). Notably, the PLA/CCPU blend films showed a significant absence of the –NCO absorption band at 2,268 cm^{-1} (Figure 1b), which indicates that IPDI has been totally reacted in the melt mixing. The absorption peak at 2,268 cm^{-1} of CCPU in the FT-IR spectra is attributed to the unreacted –NCO during the process of CCPU preparation, which is consistent with the fact.

Based on the aforementioned results, the reaction mechanism of synthetic CCPU is illustrated schematically in Figure 1c. Castor oil reacted with excess IPDI to form a short-chain molecular structure, and then curcumin and BDO were added for chain extension to obtain CCPU.

4.2 UV protection

Figure 2a gives the UV-vis light spectra of the PLA/CCPU blend films in the wavelength range of 200–800 nm. Figure 2b illustrates a comparative experiment in which the fluorescence anti-counterfeiting features on the banknote were covered by four different films (PLA, PLA/CCPU-5, –15, and –20), and then irradiated with ultraviolet light (UVB, 310 nm). The purpose of the experiment was to determine whether ultraviolet light could pass through the PLA/CCPU blend films by observing the clarity of the anti-counterfeiting marks. In the UV-vis light spectra, the pure PLA film shows a significant *T* to visible light and UV light. However, with the addition of CCPU, the PLA/CCPU blend films gradually attained a better UV-shielding ability, which exhibited the inhibition enhancement of films' UV

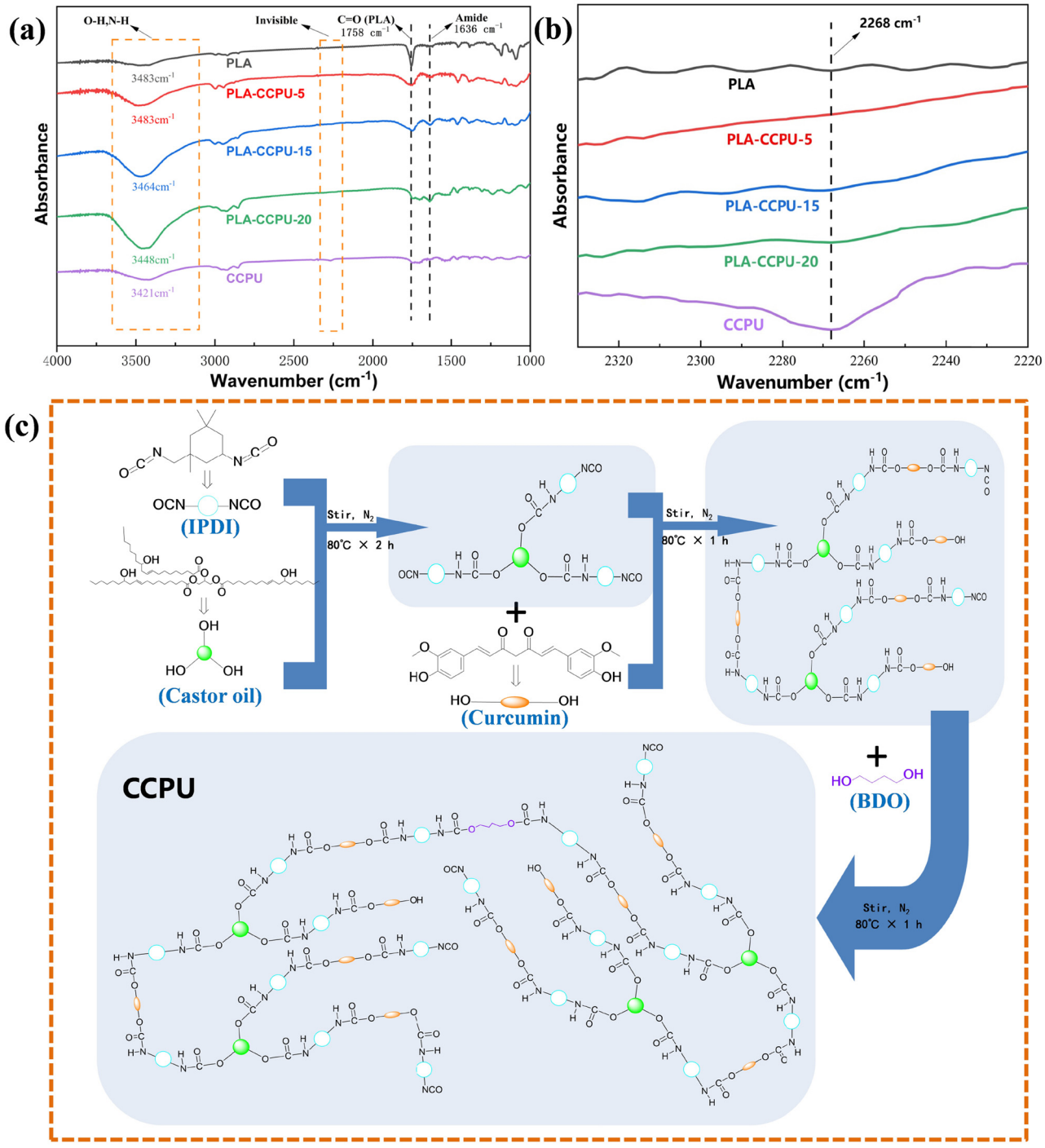

Figure 1: (a) FT-IR spectra of the CCPU and four films (PLA, PLA/CCPU-5, -15, and -20). (b) FT-IR spectra near the wavenumbers at 2,268 cm^{-1}. (c) Schematic diagram illustrating possible reaction mechanism of CCPU.

light *T* in the light wavelength range of 200–400 nm. Meanwhile, the UV light (UVB, 310 nm) could not pass through the PLA/CCPU-20 blend film, and the fluorescence anti-counterfeiting features of banknote have failed lighting by UV light in the comparative experiment (see Figure 2b, PLA/CCPU-20); it is proven that the addition of CCPU could enhance the UV-shielding ability of the PLA/CCPU blend films (60). In general, electronic excitation will be induced within curcumin structure when curcumin is exposed to solar radiation (61). In photochemical studies of UV radiation absorption, on the one hand, the electronic excitation energy is rapidly converted into vibrational energy at the

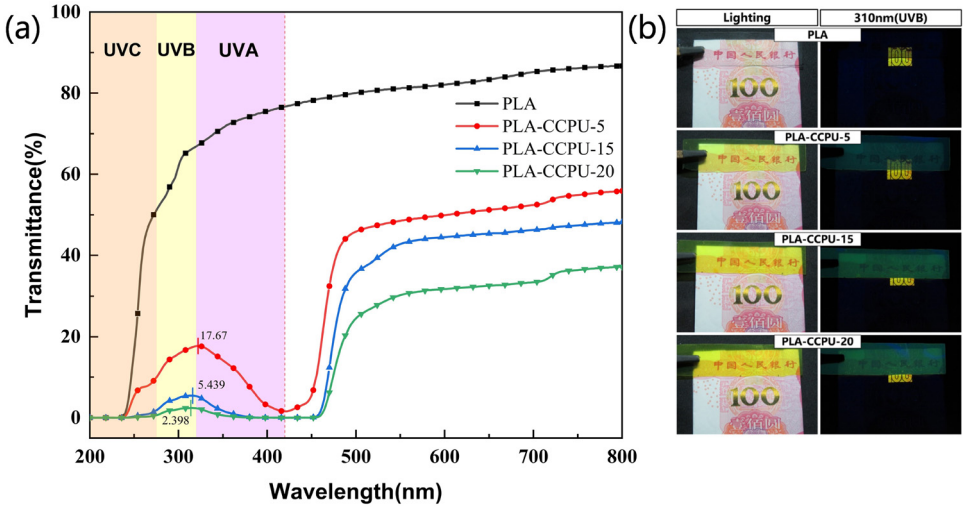

Figure 2: (a) The UV-vis spectra of the PLA/CCPU blend films (PLA, PLA/CCPU-5, -15, and -20). (b) Demonstration of UV-shielding effect by the PLA/CCPU blend films.

conjugated carbon–carbon double-bond structure and dissipated to the surroundings in the form of heat without damaging the curcumin structure (62,63); on the other hand, the hydrogen atom in hydroxyl group on the benzene ring of curcumin will transfer to the carbonyl group driven by the excitation of electrons, which may be another reason why the excitation energy of electrons is absorbed (64,65).

In conclusion, the enhanced UV-shielding capability of the PLA/CCPU blend films is attributed to the increased content of CCPU in the PLA/CCPU blends, and the core reason is the absorption of UV radiation by the conjugated carbon–carbon double-bond structure of curcumin as well as a combination of other reasons.

4.3 Optical properties

Light *T* and *H* are two important indicators for judging film's optical properties (66). Figure 3a clearly shows the variation of the PLA/CCPU blend films of light *T* and *H* (PLA, PLA/CCPU-5, -15, and -20). In the test results, the pure PLA film has high light *T* and low *H*. The PLA/CCPU blend films exhibited an *H* characteristic because of the different refractive index between PLA and CCPU (67). Moreover, with the increase of CCPU content, the *H* characteristics of the films became more pronounced. The magnified image of the PLA/CCPU blend films (Figure 3b) revealed that the increase of CCPU particles in the PLA

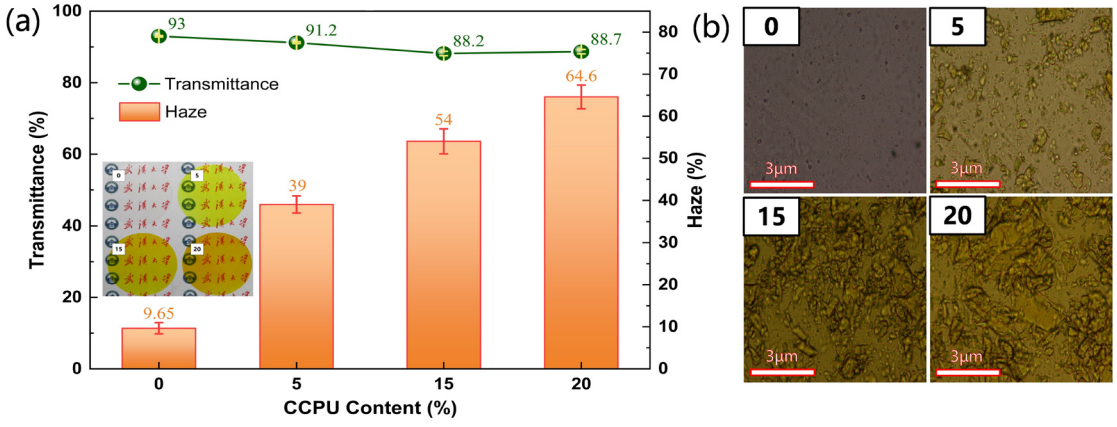

Figure 3: (a) The light *T* and *H* of the PLA/CCPU blend films. (b) The images of four films taken by electron microscopy (PLA, PLA/CCPU-5, -15, and -20).

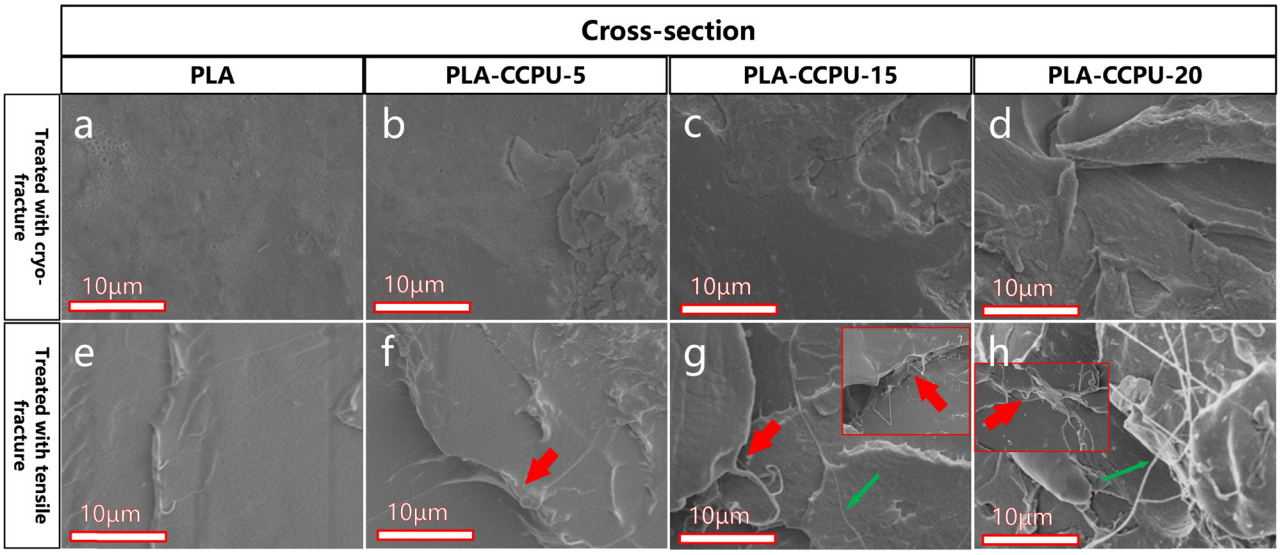

Figure 4: SEM images of the PLA and PLA/CCPU blend films' cross-section, which used different methods for treating films (treated with cryo-fracture (a–d); treated with tensile fracture (e–h)).

matrix caused the particles to be closer to each other, leading to the aggregation of particles, which resulted in an increasing number of light-scattering microregions that covered a wider area in the PLA/CCPU blend films.

4.4 Microstructural analysis

Figure 4 provides the fracture cross-sectional images of the PLA/CCPU blend films by SEM for two different treatments. One of the SEM views is a cross-sectional image of the blend films treated with cryo-fracture (Figure 4a–d), and the other is treated with tensile fracture (Figure 4e–h). The morphological structure and toughness effect of the PLA/CCPU blend films can be effectively studied. In the SEM images of Figure 4e, the smooth fracture surface observed in the pure PLA film after tensile failure indicates a typical brittle mode fracture of PLA (68). Compared with the pure PLA film, the fracture surface of the PLA/CCPU blend films becomes rougher when the CCPU content reached 5–20 wt%. Moreover, the PLA matrix of the blend

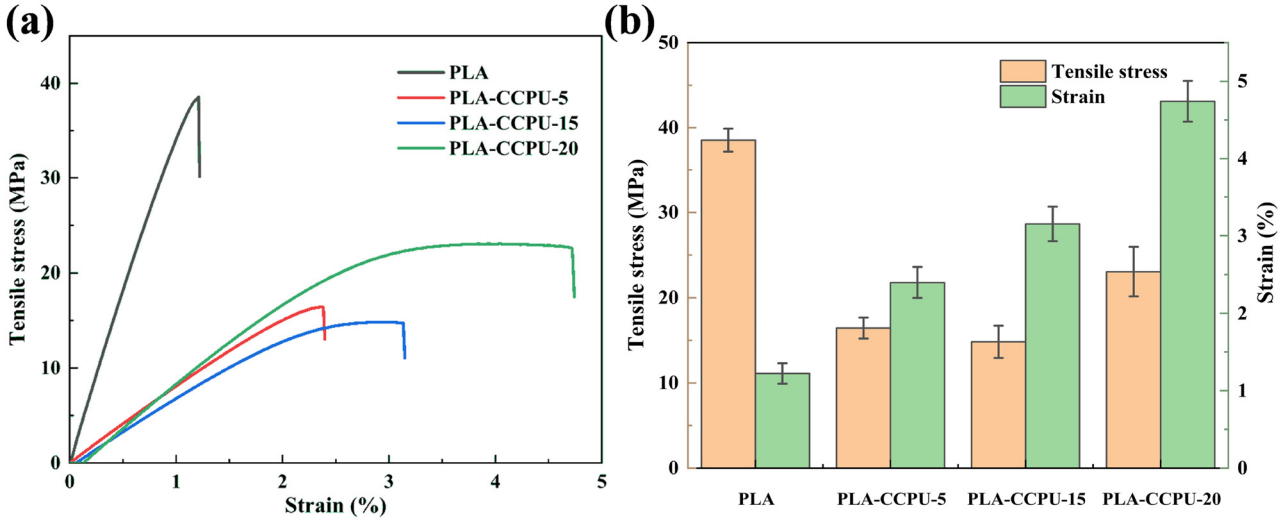

Figure 5: The tensile testing of four films (PLA, PLA/CCPU-5, -15, and -20): (a) stress–strain curves and (b) tensile strength and strain histogram to clearly observe the trend of mechanical properties of the PLA/CCPU blend films.

films appeared clearly twisted fibers (marked by the red thick arrows) arising from the fracture cross-section, and the PLA fibrous phase (marked by the green thin arrows) induced by the CCPU phase, which together indicate the characteristics of toughened fracture of the PLA/CCPU blend films (69). Meanwhile, we do not observe an obvious separation between the continuous phase (PLA) and the dispersed phase (CCPU) in the SEM images of the PLA/CCPU blend films treated with cryo-fracture (Figure 4f–h). It is indicated that the PLA and CCPU have a great interfacial compatibility (70).

4.5 Mechanical properties

The representative stress–strain curves of the PLA/CCPU blend films with different contents of CCPU are shown in Figure 5a. Pure PLA film shows a typical brittle fracture pattern in stress–strain curves, while the PLA/CCPU blend films exhibited a distinct yielding process after CCPU loaded. In Figure 5b, the elongation at break of four films (PLA, PLA/CCPU-5, -15, and -20) displayed a regular increasing trend from 1.22% to 4.74%, which shows a bit toughness improvement of the PLA film. The SEM images of their films of tensile fracture surface may also explain these mechanical testing results.

4.6 Thermal properties

Figure 6 shows the TGA and DTG thermograms to analyze the thermal stability of all PLA/CCPU blend films (PLA, PLA/CCPU-5, -15, and -20). In Figure 6a, all the blend films had a good stability (<0.8 wt% loss) between 0°C

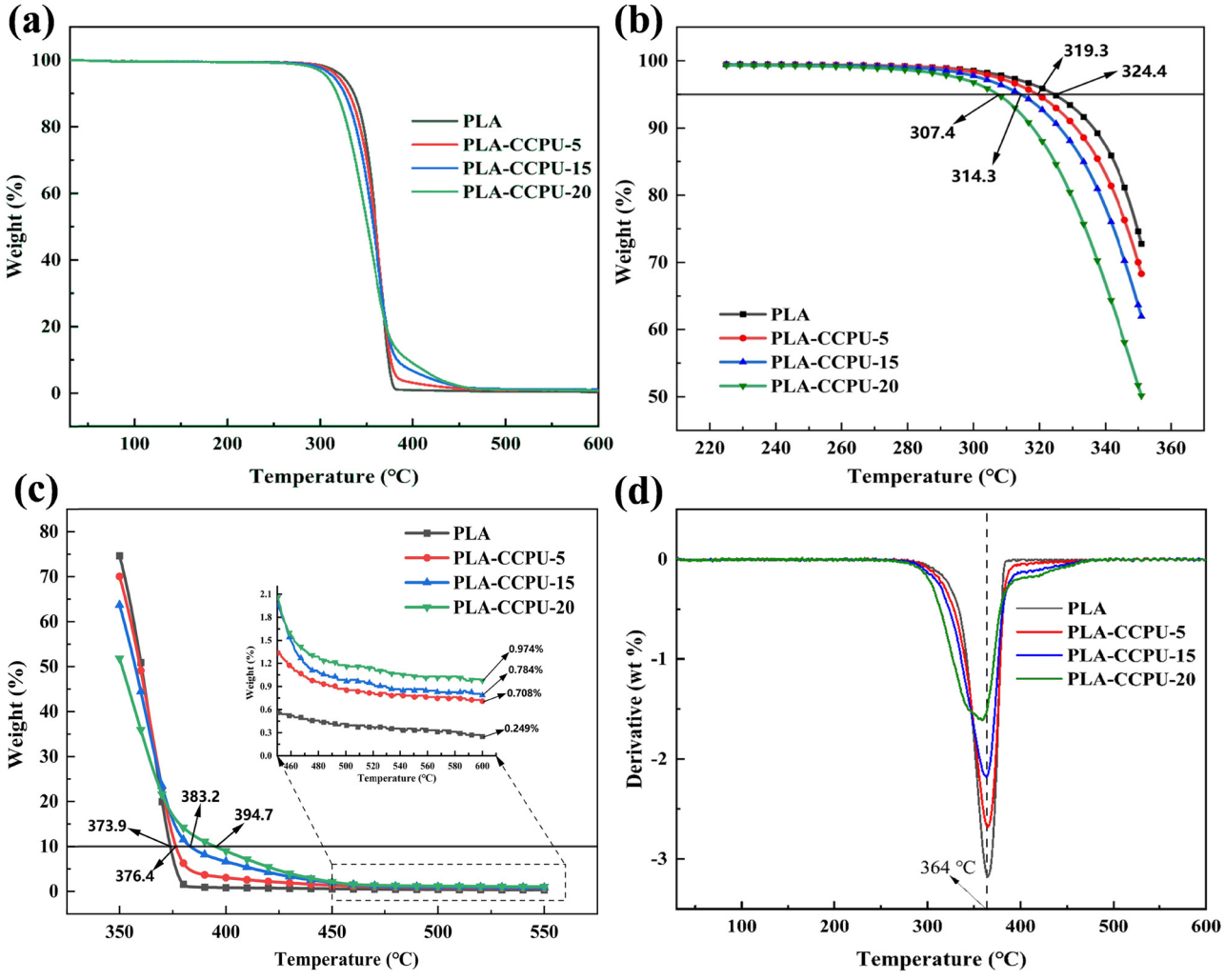

Figure 6: TG curves of the PLA/CCPU blend films (PLA, PLA/CCPU-5, -15, and -20): (a) TGA, (b) the local magnification of TGA thermogram (220–350°C), (c) the local magnification of TGA thermogram (350–550°C), and (d) DTG.

and 250°C, which provided compelling evidence that the PLA/CCPU blend films satisfy the common requirement of heat treatment.

In the range of 220–300°C, all blend films that contain the CCPU present a slow mass-losing process compared to the pure PLA film, all due to the common reason that in this work the CCPU does not have structural water and the PU bonds will start to disintegrate at 220°C (71,72). Meanwhile, in Figure 6b, the thermal stability of CCPU at the initial stage of decomposition was estimated using the temperature at which the PLA/CCPU blends lost 5 wt% (T_5) (73). In the results, it was determined that the blend films that contained more CCPU had a stronger thermal instability due to the lower temperature of T_5 for the PLA/CCPU-20 film (T_5-PLA/CCPU-20/307°C < 314°C < 319°C < 324°C). Between the 220 and 360°C range, the addition of CCPU continues to constitute a negative effect of enhanced thermal instability on the PLA/CCPU blend films.

However, the cross-linking of small amounts of curcumin on the PU backbone was demonstrated to intensify the thermal stability of PUs (74), as seen in Figure 6c for T_{90} (temperature at which 90 wt% of the blend film was lost), where the curcumin had retarded the thermal degradation of CCPU in the PLA/CCPU blend films due to the presence of benzene ring (T_{90}-PLA/CCPU-20/394°C > 383°C > 376°C > 373°C). In Figure 6d, pure PLA film and the PLA/CCPU blend films showed a maximum weight loss near 364°C, which may be related to the degradation with the PLA and the CCPU chains (75). With increasing temperature, the PLA or the CCPU that fabricated with a type of aliphatic isocyanate (IPDI) and aliphatic polyol (castor oil) both showed an almost complete degradation at 600°C (76). However, it can be seen in the enlarged view of Figure 6c that the PLA/CCPU blend films still have a mass residue close to 1%, which may be due to the residue of curcumin. This result is similar to another study that curcumin remained nearly 40% residual of mass at 600°C (21), which indirectly reflects that the curcumin was added in very small amounts inside the PLA/CCPU-20 film.

In summary, melting the CCPU with PLA could result in a UV-shielding films with favorable thermal stability, and the thermal stability of the PLA/CCPU blend films is influenced to a degree by the amount of CCPU added and the amount of curcumin added. Fortunately, despite these effects, the PLA/CCPU blend films still have an excellent thermal stability, and it is still possible to process and apply these films at high temperatures.

4.7 Interaction with water

Figure 7 illustrates a series of test results of the pure PLA film and the PLA/CCPU blend films' interaction with distilled water. Figure 7a shows the WCA details of four films (PLA, PLA/CCPU-5, -15, and -20). The WCA value of the PLA/CCPU blend films compared with that of the pure PLA film was increased from 75.62° (PLA) to 92.43° (PLA/CCPU-20) after the CCPU blended with the PLA matrix. On the one hand, the hydrophobic property of the benzene ring on curcumin molecule helped the PLA/CCPU blend films to form a micro-hydrophobic surface (77,78). On the other hand, the local cross-linking between CCPU and the PLA shortens the distance of neighboring PLA long chains in the interior of the PLA/CCPU blend films, which is another reason for the larger WCA value obtained for the PLA/CCPU blend films (79).

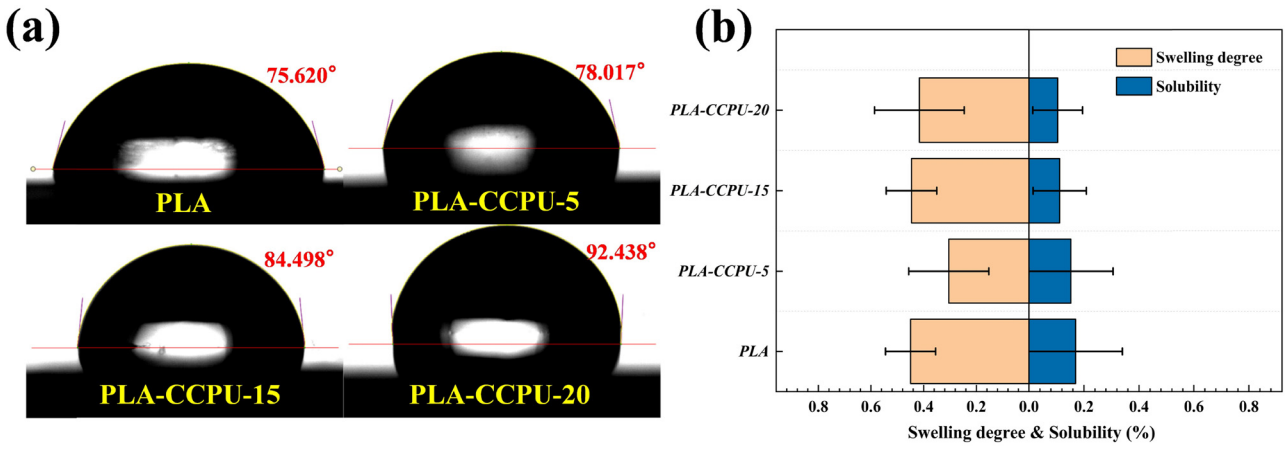

Figure 7: (a) The WCA value of the PLA/CCPU blend films (PLA, PLA/CCPU-5, -15, and -20). (b) The SD and *S* of four films (PLA, PLA/CCPU-5, -15, and -20) in distillation water.

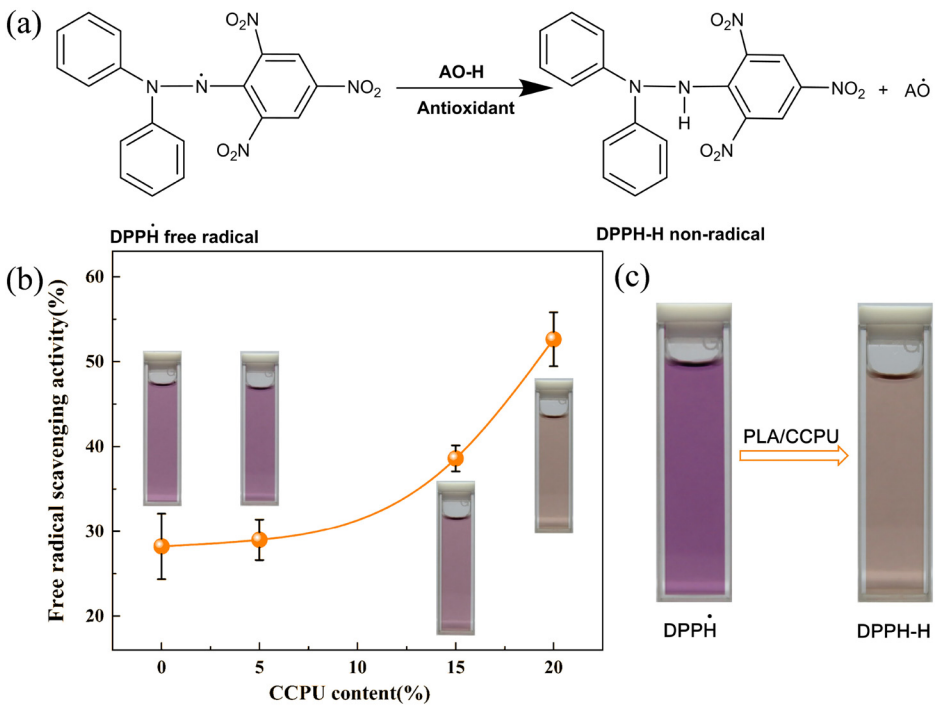

Figure 8: (a) Reaction mechanism of the DPPH with free radical scavenger. (b) The free radical scavenging activity curves of the PLA/CCPU blend films (PLA, PLA/CCPU-5, -15, and -20). (c) Discoloration of DPPH solution when the PLA/CCPU blend film was added to the DPPH solution.

Furthermore, we also tested the water SD and water *S* of each PLA/CCPU blend film (PLA, PLA/CCPU-5, -15, and -20). The test results were used to verify whether the loading of CCPU would affect the stability of the pure PLA film in distilled water (80,81). In Figure 7b, the pure PLA film and the PLA/CCPU blend films both show low water SD (<0.6 wt%) and low water *S* (<0.4 wt%). Therefore, the PLA/CCPU blend films may be applied in a humid environment, and they have higher potential to prevent the damage of film's mechanical properties caused by water swelling and water *S*.

4.8 Antioxidant activity

Figure 8a explains the principle of free radical scavengers capturing individual electrons in DPPH solution. As the amount of curcumin molecule is increased in the DPPH solution, more hydrogen radicals are provided from the curcumin and a higher number of DPPH free radicals are consequently converted to a stabilized form (DPPH-H) (82), which presents itself getting a change in solution color from purple to yellowish (Figure 8c). The degree of DPPH solution yellowing in the test can indirectly evaluate the antioxidant capacity of the PLA/CCPU blend film. In Figure 8b, the free radical scavenging rate of PLA/CCPU-20 (curcumin content 0.36 wt%) film was increased from 28% (pure PLA) to 51% (PLA/CCPU-20). Therefore, a tiny amount of curcumin was loaded to PU to obtain the CCPU, and the blended PLA with the CCPU resulted in the formation of the PLA/CCPU blend films with better antioxidant properties.

5 Conclusion

In this article, the PLA/CCPU blend films were obtained by melt mixing and compression molding. The UV-shielding ability of the PLA/CCPU blend films was significantly better than that of the pure PLA film, and the UV ray-blocking rate of the PLA/CCPU-20 film nearly achieved 97.6%. The SEM images showed that when 20 wt% CCPU was added into the PLA matrix, the fracture surface of the PLA/CCPU blend films presented a ductile fracture characteristic, and the elongation at break of four films (PLA, PLA/CCPU-5, -15, and -20) displayed a regular increasing trend from 1.22% to 4.74%. Due to the addition of CCPU and the core reason that curcumin has excellent antioxidant properties, the PLA/CCPU-20 film also showed a strong free radical scavenging rate (51%). Meanwhile, the PLA/CCPU-20 film continues to maintain a great thermal stability and moisture

resistance (WCA: 92.438°, SD: 0.4%, *S*: 0.1%) compared to the pure PLA film. Owing to the combined qualities of the PLA/CCPU blend films, such as UV-shielding, thermal stability, moisture resistance, flexibility, and anti-oxidation, the PLA/CCPU blend films may suppose to be potentially packaging films.

Funding information: This work was supported by the Nature Science Associate Foundation (NSAF) of China (Grant number: U1830127).

Author contributions: Xuya Fu: methodology, investigation, formal analysis, visualization, writing – original draft; Tao Zhang: conceptualization, writing – review and editing; Wenshuo Zhang: formal analysis, writing – review and editing; Yuye Zhong: formal analysis, visualization; Shuliang Fang: investigation, data curation; Guannan Wang: investigation, formal analysis; Ying Li: data curation; Yajun Deng: formal analysis; Xinghai Liu: resources; Houbin Li: validation, writing – review and editing, supervision.

Conflict of interest: The authors state no conflict of interest.

Data availability statement: The raw/processed data required to reproduce these findings are available from the corresponding author on a reasonable request.

References

(1) Grifoni D, Carreras G, Sabatini F, Zipoli G. UV hazard on a summer's day under Mediterranean conditions, and the protective role of a beach umbrella. Int J Biometeorol. 2005;50:75–82. doi: 10.1007/s00484-005-0278-y.

(2) Khosrovyan A, Kahru A. Evaluation of the potential toxicity of UV-weathered virgin polyamide microplastics to non-biting midge Chironomus riparius. Env Pollut. 2021;287:117334. doi: 10.1016/j.envpol.2021.117334.

(3) Basumatary IB, Mukherjee A, Katiyar V, Kumar S. Biopolymer-based nanocomposite films and coatings: recent advances in shelf-life improvement of fruits and vegetables. Crit Rev Food Sci Nutr. 2022;62:1912–35. doi: 10.1080/10408398.2020.1848789.

(4) Calvo ME, Castro Smirnov JR, Míguez H. Novel approaches to flexible visible transparent hybrid films for ultraviolet protection. J Polym Sci Part B: Polym Phys. 2012;50:945–56. doi: 10.1002/polb.23087.

(5) Egambaram OP, Kesavan Pillai S, Ray SS. Materials science challenges in skin UV protection: A review. Photochem Photobiol. 2020;96:779–97. doi: 10.1111/php.13208.

(6) Lu T, Solis-Ramos E, Yi Y, Kumosa M. UV degradation model for polymers and polymer matrix composites. Polym Degrad Stabil. 2018;154:203–10. doi: 10.1016/j.polymdegradstab.2018.06.004.

(7) Moustafa H, Youssef AM, Darwish NA, Abou-Kandil AI. Eco-friendly polymer composites for green packaging: Future vision and challenges. Compos Part B-Engineering. 2019;172:16–25. doi: 10.1016/j.compositesb.2019.05.048.

(8) Zhao L, Duan G, Zhang G, Yang H, He S, Jiang S. Electrospun functional materials toward food packaging applications: A review. Nanomaterials (Basel). 2020;10(1):150. doi: 10.3390/nano10010150.

(9) Wallis C. Terrestrial fugitive plastic packaging: the blind spot in resolving plastic pollution. Green Mater. 2020;8:3–5. doi: 10.1680/jgrma.19.00044.

(10) Jambeck JR, Geyer R, Wilcox C, Siegler TR, Perryman M, Andrady A, et al. Plastic waste inputs from land into the ocean. Science. 2015;347:768–71. doi: 10.1126/science.1260352.

(11) Rojas A, Velasquez E, Patino Vidal C, Guarda A, Galotto MJ, Lopez de Dicastillo C. Active PLA packaging films: Effect of processing and the addition of natural antimicrobials and antioxidants on physical properties, release kinetics, and compostability. Antioxid (Basel). 2021;10(12):1976. doi: 10.3390/antiox10121976.

(12) Pang B, Wu Z-Y, Wang Z-B, You B-Q, Guo Y-R, Li S, et al. Design of a ZnO@ plant polyphenol/poly (vinyl alcohol) film via plant polyphenol-induced cross-linking and its enhanced UV shielding and antibacterial performance. ACS Sustain Chem Eng. 2022;10:9369–80. doi: 10.1021/acssuschemeng.2c01444.

(13) Zhang Y, Naebe M. Lignin: A review on structure, properties, and applications as a light-colored UV absorber. ACS Sustain Chem Eng. 2021;9:1427–42. doi: 10.1021/acssuschemeng.0c06998.

(14) Yang H, Shi B, Xue Y, Ma Z, Liu L, Liu L, et al. Molecularly engineered lignin-derived additives enable fire-retardant, UV-shielding, and mechanically strong polylactide biocomposites. Biomacromolecules. 2021;22:1432–44. doi: 10.1021/acs.biomac.0c01656.

(15) Sadeghifar H, Venditti R, Jur J, Gorga RE, Pawlak JJ. Cellulose-lignin biodegradable and flexible UV protection film. ACS Sustain Chem Eng. 2016;5:625–31. doi: 10.1021/acssuschemeng.6b02003.

(16) Chandrappa H, Bhajantri RF, Prarthana N. Simple fabrication of PVA-ATE (Amaranthus tricolor leaves extract) polymer biocomposites: An efficient UV-Shielding material for organisms in terrestrial and aquatic ecosystems. Optical Mater. 2020;109:110204. doi: 10.1016/j.optmat.2020.110204.

(17) Liu J, Wang H, Wang P, Guo M, Jiang S, Li X, et al. Films based on κ-carrageenan incorporated with curcumin for freshness monitoring. Food Hydrocoll. 2018;83:134–42. doi: 10.1016/j.foodhyd.2018.05.012.

(18) Miglioranza BMG, Spinelli FR, Stoffel F, Piemolini-Barreto LT. Biodegradable film for raisins packaging application: Evaluation of physico-chemical characteristics and antioxidant potential. Food Chem. 2021;365:130538. doi: 10.1016/j.foodchem.2021.130538.

(19) Prasad S, DuBourdieu D, Srivastava A, Kumar P, Lall R. Metal-curcumin complexes in therapeutics: An approach to enhance pharmacological effects of curcumin. Int J Mol Sci. 2021;22(13):7094. doi: 10.3390/ijms22137094.

(20) Rai M, Pandit R, Gaikwad S, Yadav A, Gade A. Potential applications of curcumin and curcumin nanoparticles: from

traditional therapeutics to modern nanomedicine. Nanotechnol Rev. 2015;4:161–72. doi: 10.1515/ntrev-2015-0001.
(21) Qiao YC, Duan LJ. Curcumin-loaded polyvinyl butyral film with antibacterial activity. e-Polymers. 2020;20:673–81. doi: 10.1515/epoly-2020-0042.
(22) Kim S, Choi K. Occurrences, toxicities, and ecological risks of benzophenone-3, a common component of organic sunscreen products: a mini-review. Env Int. 2014;70:143–57. doi: 10.1016/j.envint.2014.05.015.
(23) Castillo ML, López-Tobar E, Sanchez-Cortes S, Flores G, Blanch GP. Stabilization of curcumin against photodegradation by encapsulation in gamma-cyclodextrin: A study based on chromatographic and spectroscopic (Raman and UV-visible) data. Vibrational Spectrosc. 2015;81:106–11. doi: 10.1016/j.vibspec.2015.10.008.
(24) Chopra D, Ray L, Dwivedi A, Tiwari SK, Singh J, Singh KP, et al. Photoprotective efficiency of PLGA-curcumin nanoparticles versus curcumin through the involvement of ERK/AKT pathway under ambient UV-R exposure in HaCaT cell line. Biomaterials. 2016;84:25–41. doi: 10.1016/j.biomaterials.2016.01.018.
(25) Kang J, Kim YH, Choi SJ, Rho SJ, Kim YR. Improving the stability and curcumin retention rate of curcumin-loaded filled hydrogel prepared using 4alphaGTase-treated rice starch. Foods. 2021;10(1):150. doi: 10.3390/foods10010150.
(26) Zdyrko B, Swaminatha Iyer K, Luzinov I. Macromolecular anchoring layers for polymer grafting: comparative study. Polymer. 2006;47:272–9. doi: 10.1016/j.polymer.2005.11.029.
(27) Lee B, Maher MJ, Schibur HJ, Hillmyer MA, Bates FS. Toughening polylactide with graft-block polymers. Acs Appl Polym Mater. 2022;4:3408–16. doi: 10.1021/acsapm.2c00036.
(28) Zhang T, Deng Y, Zhang W, Wang G, Zhong Y, Su C, et al. A self-colored waterborne polyurethane film with natural curcumin as a chain extender and excellent UV-Absorbing properties. Polymer. 2022;239:124465. doi: 10.1016/j.polymer.2021.124465.
(29) Zhang T, Zhang W, Deng Y, Chu Y, Zhong Y, Wang G, et al. Curcumin-based waterborne polyurethane-gelatin composite bioactive films for effective UV shielding and inhibition of oil oxidation. Food Control. 2022;141:109199. doi: 10.1016/j.foodcont.2022.109199.
(30) Mahmood K, Zia KM, Zuber M, Salman M, Anjum MN. Recent developments in curcumin and curcumin based polymeric materials for biomedical applications: A review. Int J Biol Macromol. 2015;81:877–90. doi: 10.1016/j.ijbiomac.2015.09.026.
(31) Ma QY, Du L, Wang LJ. Tara gum/polyvinyl alcohol-based colorimetric NH3 indicator films incorporating curcumin for intelligent packaging. Sens Actuators B-Chemical. 2017;244:759–66. doi: 10.1016/j.snb.2017.01.035.
(32) Feng Y, Xiao K, He Y, Du B, Hong J, Yin H, et al. Tough and biodegradable polyurethane-curcumin composited hydrogel with antioxidant, antibacterial and antitumor properties. Mater Sci Eng C Mater Biol Appl. 2021;121:111820. doi: 10.1016/j.msec.2020.111820.
(33) Mahmood K, Noreen I, Riaz M, Zuber M, Salman M, Rehman S, et al. Synthesis and characterization of novel curcumin based polyurethanes varying diisocyanates structure. J Polym Res. 2016;23:1–9. doi: 10.1007/s10965-016-1125-z.
(34) Zia F, Zia KM, Zuber M, Rehman S, Tabasum S, Sultana S. Synthesis and characterization of chitosan/curcumin blends based polyurethanes. Int J Biol Macromol. 2016;92:1074–81. doi: 10.1016/j.ijbiomac.2016.08.005.
(35) Pavlopoulou E, Chrissopoulou K, Pispas S, Hadjichristidis N, Anastasiadis SH. The micellization of well-defined single graft copolymers in block copolymer/homopolymer blends. Polym (Basel). 2021;13(5):833. doi: 10.3390/polym13050833.
(36) Shlosman K, Suckeveriene RY, Rosen-Kligvasser J, Tchoudakov R, Zelikman E, Semiat R, et al. Controlled migration of antifog additives from LLDPE compatibilized with LLDPE grafted maleic anhydride. Polym Adv Technol. 2014;25:1484–91. doi: 10.1002/pat.3390.
(37) Liu T, Zhang HM, Zuo M, Zhang WJ, Zhu WP, Zheng Q. Selective location and migration of poly(methyl methacrylate)- grafted clay nanosheets with low grafting density in poly(methyl methacrylate)/poly (styrene-co-acrylonitrile) blends. Compos Sci Technol. 2019;169:110–9. doi: 10.1016/j.compscitech.2018.11.021.
(38) Garlotta D. A literature review of poly(lactic acid). J Polym Environ. 2001;9:63–84. doi: 10.1023/a:1020200822435.
(39) Sha L, Chen Z, Chen Z, Zhang A, Yang Z. Polylactic acid based nanocomposites: Promising safe and biodegradable materials in biomedical field. Int J Polym Sci. 2016;2016:1–11. doi: 10.1155/2016/6869154.
(40) Armentano I, Bitinis N, Fortunati E, Mattioli S, Rescignano N, Verdejo R, et al. Multifunctional nanostructured PLA materials for packaging and tissue engineering. Prog Polym Sci. 2013;38:1720–47. doi: 10.1016/j.progpolymsci.2013.05.010.
(41) Park JW, Shin JH, Shim GS, Sim KB, Jang SW, Kim HJ. Mechanical strength enhancement of polylactic acid hybrid composites. Polym (Basel). 2019;11(2):349. doi: 10.3390/polym11020349.
(42) Lasprilla AJ, Martinez GA, Lunelli BH, Jardini AL, Filho RM. Polylactic acid synthesis for application in biomedical devices - a review. Biotechnol Adv. 2012;30:321–8. doi: 10.1016/j.biotechadv.2011.06.019.
(43) Zhao X, Liu J, Li J, Liang X, Zhou W, Peng S. Strategies and techniques for improving heat resistance and mechanical performances of poly(lactic acid) (PLA) biodegradable materials. Int J Biol Macromol. 2022;218:115–34. doi: 10.1016/j.ijbiomac.2022.07.091.
(44) Mestdagh F, De Meulenaer B, De Clippeleer J, Devlieghere F, Huyghebaert A. Protective influence of several packaging materials on light oxidation of milk. J Dairy Sci. 2005;88:499–510. doi: 10.3168/jds.S0022-0302(05)72712-0.
(45) Auras R, Harte B, Selke S. An overview of polylactides as packaging materials. Macromol Biosci. 2004;4:835–64. doi: 10.1002/mabi.200400043.
(46) Wang J, Han X, Zhang C, Liu K, Duan G. Source of nanocellulose and its application in nanocomposite packaging material: A review. Nanomaterials (Basel). 2022;12(18):3158. doi: 10.3390/nano12183158.
(47) Liu L, Xu Y, Pan Y, Xu M, Di Y, Li B. Facile synthesis of an efficient phosphonamide flame retardant for simultaneous enhancement of fire safety and crystallization rate of poly (lactic acid). Chem Eng J. 2021;421:127761. doi: 10.1016/j.cej.2020.127761.
(48) Wang C, Gong C, Qin Y, Hu Y, Jiao A, Jin Z, et al. Bioactive and functional biodegradable packaging films reinforced with

nanoparticles. J Food Eng. 2022;312:110752. doi: 10.1016/j.jfoodeng.2021.110752.
(49) Qi X, Ren Y, Wang X. New advances in the biodegradation of Poly(lactic) acid. Int Biodeterior Biodegrad. 2017;117:215–23. doi: 10.1016/j.ibiod.2017.01.010.
(50) Milovanovic S, Pajnik J, Lukic I. Tailoring of advanced poly (lactic acid)-based materials: A review. J Appl Polym Sci. 2021;139(12):51839. doi: 10.1002/app.51839.
(51) Nagarajan V, Mohanty AK, Misra M. Perspective on polylactic acid (PLA) based sustainable materials for durable applications: Focus on toughness and heat resistance. ACS Sustain Chem Eng. 2016;4:2899–916. doi: 10.1021/acssuschemeng.6b00321.
(52) Jiang S, Sun H, Wang H, Ladewig BP, Yao Z. A comprehensive review on the synthesis and applications of ion exchange membranes. Chemosphere. 2021;282:130817. doi: 10.1016/j.chemosphere.2021.130817.
(53) Guo Z, Wang ZB, Qin YJ, Zhang JT, Qi Y, Liu BG, et al. Fabrication of biodegradable nanofibers via melt extrusion of immiscible blends. e-Polymers. 2022;22:733–41. doi: 10.1515/epoly-2022-0059.
(54) Blanco I, Siracusa V. Kinetic study of the thermal and thermo-oxidative degradations of polylactide-modified films for food packaging. J Therm Anal Calorim. 2012;112:1171–7. doi: 10.1007/s10973-012-2535-8.
(55) Khan A, Naveed M, Rabnawaz M. Melt-reprocessing of mixed polyurethane thermosets. Green Chem. 2021;23:4771–9. doi: 10.1039/d1gc01232k.
(56) Gürler N, Paşa S, Temel H. Silane doped biodegradable starch-PLA bilayer films for food packaging applications: Mechanical, thermal, barrier and biodegradability properties. J Taiwan Inst Chem Eng. 2021;123:261–71. doi: 10.1016/j.jtice.2021.05.030.
(57) Yang CX, Tang HB, Wang YF, Liu Y, Wang J, Shi WZ, et al. Development of PLA-PBSA based biodegradable active film and its application to salmon slices. Food Packaging Shelf Life. 2019;22:100393. doi: 10.1016/j.fpsl.2019.100393.
(58) Xu A, Wang Y, Gao J, Wang J. Facile fabrication of a homogeneous cellulose/polylactic acid composite film with improved biocompatibility, biodegradability and mechanical properties. Green Chem. 2019;21:4449–56. doi: 10.1039/c9gc01918a.
(59) Liu H, Chen N, Shan P, Song P, Liu X, Chen J. Toward fully bio-based and supertough PLA blends via in situ formation of cross-linked biopolyamide continuity network. Macromolecules. 2019;52:8415–29. doi: 10.1021/acs.macromol.9b01398.
(60) Zheng Q, Huang J, Li H, Chen L. Preparation of highly visible transparent ZnO/cellophane UV-shielding film by RF magnetron sputtering. Ceram Int. 2019;45:3729–34. doi: 10.1016/j.ceramint.2018.11.038.
(61) Karsili TN, Marchetti B, Ashfold MN, Domcke W. Ab initio study of potential ultrafast internal conversion routes in oxybenzone, caffeic acid, and ferulic acid: implications for sunscreens. J Phys Chem A. 2014;118:11999–2010. doi: 10.1021/jp507282d.
(62) Tuna D, Sobolewski AL, Domcke W. Photochemical mechanisms of radiationless deactivation processes in urocanic acid. J Phys Chem B. 2014;118:976–85. doi: 10.1021/jp411818j.
(63) Zayat M, Garcia-Parejo P, Levy D. Preventing UV-light damage of light sensitive materials using a highly protective UV-absorbing coating. Chem Soc Rev. 2007;36:1270–81. doi: 10.1039/b608888k.
(64) Xiao JP, Li Y. Screening of benzophenone ultraviolet absorbers with high-efficiency light absorption capacity, low-permeability and low-toxicity by 3D-QSAR model. J Mol Liq. 2022;347:118364. doi: 10.1016/j.molliq.2021.118364.
(65) Shamoto Y, Yagi M, Oguchi-Fujiyama N, Miyazawa K, Kikuchi A. Photophysical properties of hexyl diethylaminohydroxybenzoylbenzoate (Uvinul A Plus), a UV-A absorber. Photochem Photobiol Sci. 2017;16:1449–57. doi: 10.1039/c7pp00164a.
(66) Menamparambath MM, Yang K, Kim HH, Bae OS, Jeong MS, Choi JY, et al. Reduced haze of transparent conductive films by smaller diameter silver nanowires. Nanotechnology. 2016;27:465706. doi: 10.1088/0957-4484/27/46/465706.
(67) Preston C, Xu Y, Han X, Munday JN, Hu L. Optical haze of transparent and conductive silver nanowire films. Nano Res. 2013;6:461–8. doi: 10.1007/s12274-013-0323-9.
(68) Yang R, Cao H, Zhang P, Chen L, Zou G, Zhang X, et al. Highly toughened and heat-resistant poly(lactic acid) with balanced strength using an unsaturated liquid crystalline polyester via dynamic vulcanization. ACS Appl Polym Mater. 2020;3:299–309. doi: 10.1021/acsapm.0c01095.
(69) Zhang Y, Jing J, Liu T, Xi LD, Sai T, Ran SY, et al. A molecularly engineered bioderived polyphosphate for enhanced flame retardant, UV-blocking and mechanical properties of poly(lactic acid). Chem Eng J. 2021;411:128493. doi: 10.1016/j.cej.2021.128493.
(70) He L, Song F, Li D-F, Zhao X, Wang X-L, Wang Y-Z. Strong and tough polylactic acid based composites enabled by simultaneous reinforcement and interfacial compatibilization of microfibrillated cellulose. ACS Sustain Chem Eng. 2020;8:1573–82. doi: 10.1021/acssuschemeng.9b06308.
(71) Chiang M-F, Wu T-M. Intercalation of γ-PGA in Mg/Al layered double hydroxides: An in situ WAXD and FTIR investigation. Appl Clay Sci. 2011;51:330–4. doi: 10.1016/j.clay.2010.12.021.
(72) Oprea S. Synthesis and properties of polyurethane elastomers with castor oil as crosslinker. J Am Oil Chemists' Soc. 2009;87:313–20. doi: 10.1007/s11746-009-1501-5.
(73) Stirna U, Lazdina B, Vilsone D, Lopez MJ, Vargas-Garcia MD, Suarez-Estrella F, et al. Structure and properties of the polyurethane and polyurethane foam synthesized from castor oil polyols. J Cell Plast. 2012;48:476–88. doi: 10.1177/0021955x12445178.
(74) Shah SAA, Athir N, Imran M, Cheng J, Zhang JY. Thermo-mechanically improved curcumin and zwitterion incorporated polyurethane-urea elastomers. Polym Degrad Stabil. 2019;164:28–35. doi: 10.1016/j.polymdegradstab.2019.03.018.
(75) Lim LT, Auras R, Rubino M. Processing technologies for poly (lactic acid). Prog Polym Sci. 2008;33:820–52. doi: 10.1016/j.progpolymsci.2008.05.004.
(76) Ionescu M, Radojcic D, Wan XM, Shrestha ML, Petrovic ZS, Upshaw TA. Highly functional polyols from castor oil for rigid polyurethanes. Eur Polym J. 2016;84:736–49. doi: 10.1016/j.eurpolymj.2016.06.006.
(77) Wang JC, Wu YK, Cao YJ, Li GS, Liao YF. Influence of surface roughness on contact angle hysteresis and spreading work. Colloid Polym Sci. 2020;298:1107–12. doi: 10.1007/s00396-020-04680-x.

(78) Zhang W, Zhang T, Deng Y, Guan Z, Zhong Y, Fang S, et al. Environmentally friendly gelatin-based ink with durability on low surface energy substrates for anti-counterfeiting printing. J Clean Prod. 2022;362:132518. doi: 10.1016/j.jclepro.2022.132518.
(79) Roy S, Rhim JW. Carboxymethyl cellulose-based antioxidant and antimicrobial active packaging film incorporated with curcumin and zinc oxide. Int J Biol Macromol. 2020;148:666–76. doi: 10.1016/j.ijbiomac.2020.01.204.
(80) Datta D, Halder G. Effect of media on degradability, physico-mechanical and optical properties of synthesized polyolefinic and PLA film in comparison with casted potato/corn starch biofilm. Process Saf Environ Prot. 2019;124:39–62. doi: 10.1016/j.psep.2019.02.002.
(81) Kluver E, Baltzer M, Langer A, Meyer M. Additive manufacturing with thermoplastic collagen. Polym (Basel). 2022;14(5):974. doi: 10.3390/polym14050974.
(82) Cvek M, Paul UC, Zia J, Mancini G, Sedlarik V, Athanassiou A. Biodegradable films of PLA/PPC and curcumin as packaging materials and smart indicators of food spoilage. ACS Appl Mater Interfaces. 2022;14:14654–67. doi: 10.1021/acsami.2c02181.